ELSEVIER

Polymer 42 (2001) 1561–1566

polymer

www.elsevier.nl/locate/polymer

Direct observation of interfacial profiles of polymer gels during the phase transition by Raman microimaging

R. Appel[a], T.W. Zerda[a,*], C. Wang[b], Z. Hu[b]

[a]*Department of Physics and Astronomy, Texas Christian University, TCU Box 298840, Fort Worth, TX 76129, USA*
[b]*Department of Physics, University of North Texas, Denton, TX 76203, USA*

Received 28 February 2000; received in revised form 12 July 2000; accepted 12 July 2000

Abstract

The interface profiles between *N*-isopropylacrylamide (NIPA) hydrogel and water have been directly observed using Raman microimaging technique. As the NIPA hydrogel undergoes the volume phase transition, it is found that the interface becomes thicker and smoother. Specifically, the average interfacial thickness of the NIPA gel at room temperature is about 37 μm, but increases to 65 μm at 37°C, the temperature that is higher than the phase transition temperature of $T_c = 34$°C. The thicker interface may be related to a dense shell formation during the gel shrinking process. The decrease in surface roughness is probably related to hydrophobic properties of the gel at $T > T_c$. The repulsive energy between water and the polymer is minimized when the total surface of the interface is reduced, a process, which results in a smoother surface.

Keywords: Raman spectroscopy; Imaging; Polymer interface

1. Introduction

The interface profile may affect mechanical properties, kinetics of surface adhesion and absorption, wetting, biocompatibility, and optical properties of a large variety of materials. Extensive efforts have been directed to understanding interfacial properties of biopolymers and biomaterials [1]. In this paper, we report for the first time direct observations of the interfacial profile between the *N*-isopropylacrylamide (NIPA) hydrogel and water below and above the volume phase transition temperature of the NIPA gel using Raman microimaging technique.

Hydrogels are a unique class of macromolecular networks that can contain a large fraction of water within their structure. They are particularly suitable for biomedical applications because of their ability to simulate biological tissues [2]. In response to environmental stimuli such as temperature and pH, some hydrogels can change their volume by three orders of magnitude [3,4]. NIPA is one of these environmentally responsive hydrogels and undergoes the volume phase transition at 34°C [5]. Various surface patterns caused by mechanical instability and constraints have been studied during NIPA gel swelling or shrinking processes [6–8].

Theoretical models of interfacial properties depend on experimental profiles, therefore, providing reliable data is a key factor. Such data are available for metals and other solid surfaces but information is scarce for the water–hydrogel interface. This is because many experimental techniques do not work well in the presence of water. Conventional electron microscope techniques have been used in the past, but results obtained, although informative and important, are not completely reliable because the inherent pore structure cannot be preserved during the sample preparation. For example, the freeze-dry method used by some researchers often leads to the collapse of the pore structure due to ice formation and/or volatile evaporation in vacuum [9]. As a result, most current studies on hydrogels involved investigation of the morphology of the exterior surface using optical microscope [6–8] and atomic force microscopy [10]. We have recently developed Raman microimaging technique for direct observation of hydrogel structures [11].

2. Experimental

The NIPA gel samples were made by free radical polymerization. A mixture of 690 mM of NIPA monomer, 8.6 mM of methylene-bis-acrylamide as a crosslinker, and 240 μl of tetramethylethylene-diamine as an accelerator was dissolved in 100 ml of deionized and distilled water. Nitrogen gas was bubbled through the solution to remove

* Corresponding author. Tel.: +1-817-257-7375; fax: +1-817-257-7742.
E-mail address: t.zerda@tcu.edu (T.W. Zerda).

0032-3861/01/$ - see front matter
PII: S0032-3861(00)00544-9

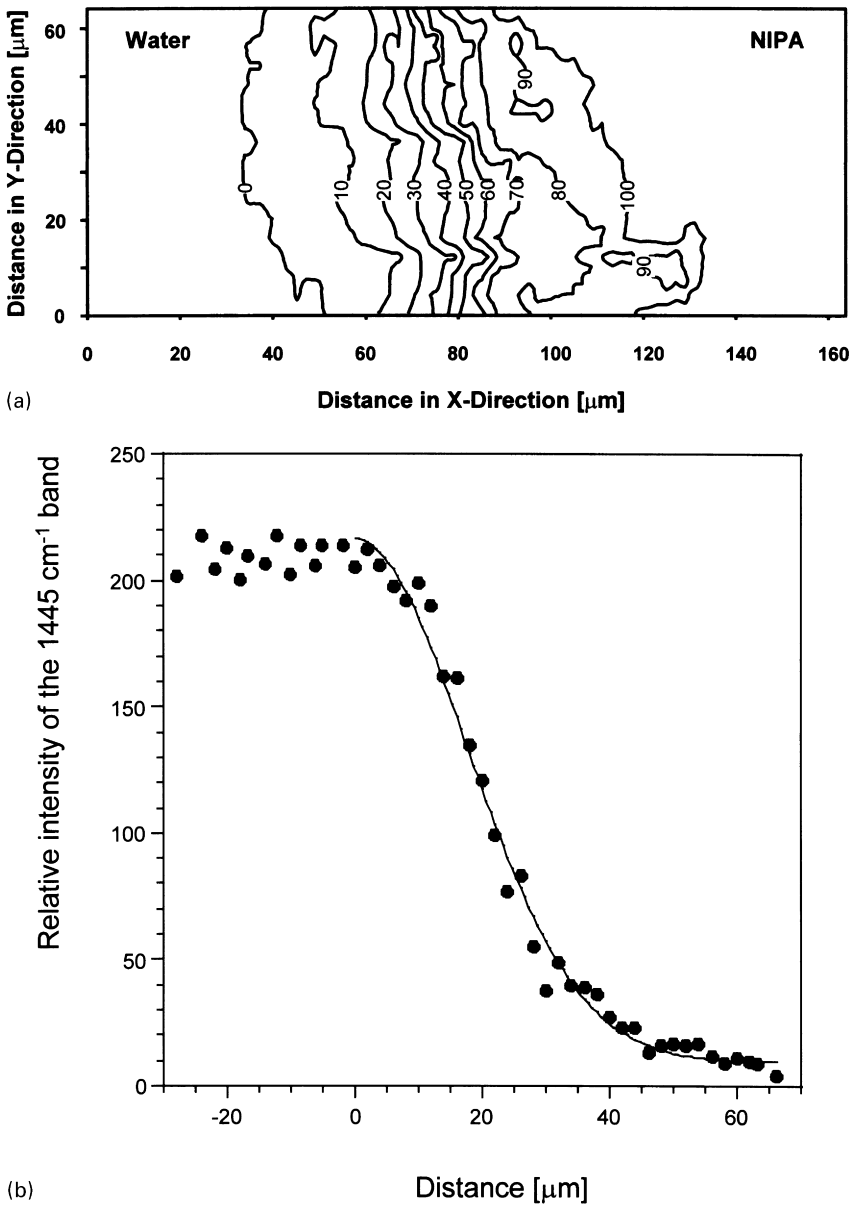

Fig. 1. (a) Distribution of the NIPA gel, obtained from Raman band intensity, near the gel boundary with water at $T = 22°C$. The contour lines were normalized to 100. (b) Circles: Raman intensity of the 1445 cm^{-1} band along a straight line perpendicular to the water–gel interface at $T = 22°C$. The solid line represents the best fit of a Gaussian function, Eq. (1), to the experimental points. The interfacial thickness, $d = 25.6$ μm.

dissolved oxygen. Ammonium persulfate (0.169 mM) was added to the solution as an initiator. Then the solution was poured between two microscope slides with spacing of 2.0 mm in a nitrogen environment. The molecular number ratio of the NIPA monomer to the BIS crosslinker was about 80:1. There were about 40 monomer molecules, or about 80 backbone C–C bonds, between two crosslinkers. Assuming that the chains were fully extended in water at room temperature, the mesh size of the NIPA polymer network was estimated about 10 nm.

The Raman microimaging system consists of an argon ion laser operating at 514 nm, a confocal microscope with 100× objective, an *x*–*y*–*z*-micropositioning stage, a spectrograph equipped with a notch filter and transmissive holographic gratings, and a CCD camera. The gel was placed inside a specially designed holder kept at constant temperature. The temperature was stable within 0.1°C. To prevent water evaporation, the sample holder was covered with a 0.1 mm thick microscope slide. The holder was mounted onto a positioning stage and advanced in steps of 1 μm in the lateral directions. The size of the step was selected to be larger than the spatial resolution of the microscope −0.5 μm. As the laser scanned the sample, for each step, we recorded Raman spectra in the range from 300 to 2000 cm^{-1}. The spectral resolution of the instrument was 1.5 cm^{-1}. The laser power at the gel surface was 0.1 W.

The outer surfaces of the gel slabs were measured after they were detached from the microslides and extensively

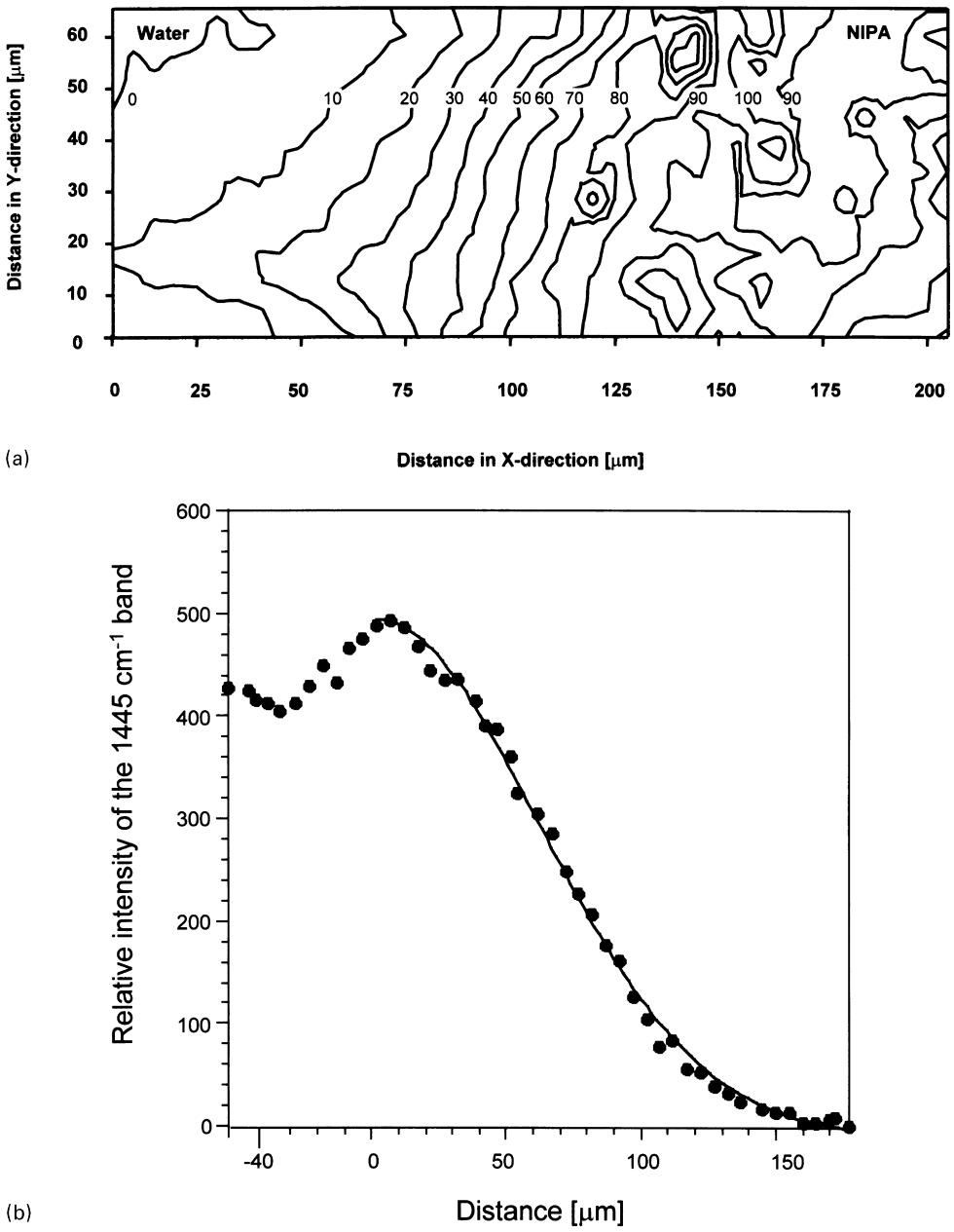

Fig. 2. (a) Distribution of the NIPA gel near the interface when the sample was heated to 37°C. The contour lines were normalized to 100. (b) Circles: Raman intensity of the 1445 cm^{-1} band along a straight line perpendicular to the water–gel interface at $T = 37$°C. The solid line represents the best fit of a Gaussian function, Eq. (1), to the experimental points on the left side of the interface. The origin was placed at the maximum density of the interface. The interfacial thickness, $d = 65.3$ μm.

washed with deionized and distilled water to remove residual chemicals. The laser was focused just below the surface of the gel and linear scans were run in the direction perpendicular to the interface. We measured the intensity of the 1445 cm^{-1} peak assigned to the CH_2 bending vibration [11]. We assumed that the measured intensity was proportional to the concentration of the polymer within the focus of the laser. A set of parallel scans formed a two-dimensional image of the water–gel interface. The Raman measurements were performed for ten samples and they showed reproducible results.

3. Results and discussion

The contour map shown in Fig. 1(a) illustrates how the density of NIPA varied across the interface at room temperature. It is seen that the boundary is not well defined and the polymer extends into water to various depths. Although to a naked eye the surface looks smooth, Fig. 1(a) clearly indicates that the surface is not homogenous. We also measured the interfaces that were cut with a razor blade and thus were not in contact with the glass during the gelation process. The results were similar to those interfaces

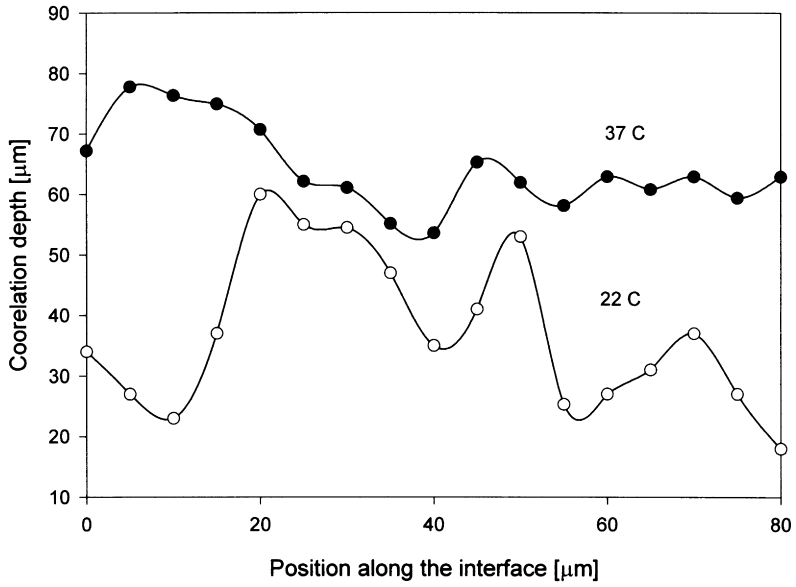

Fig. 3. Fluctuations in the correlation depth, which measures the interfacial thickness of the NIPA gel at 22°C (open circles) and 37°C (filled circles).

which were in contact with the glass. Therefore, interface profiles revealed by Raman microimaging are not related to the glass substrate.

Experimental points obtained during the linear scans (Fig. 1(a) is a composition of such scan lines) were fitted to a Gaussian distribution function

$$F(x) = c_1 + c_2 \exp(-x^2/d^2) \quad (1)$$

where x measures linear displacement perpendicular to the interface and d, the correlation depth, is the fitting parameter. The correlation depth parameter is a measure of the thickness of the interface at the location of the scan-line. Eq. (1) fitted experimental data very well as shown in Fig. 1(b). Because the interface is not uniform, different scans provided various d values. The average interface thickness is 37 ± 23 μm at room temperature.

Fig. 2(a) shows the contour map for the NIPA–water interface at 37°C. Comparing Fig. 2(a) with Fig. 1(a) one can see that the surface became less irregular as the gel was heated above its transition temperature at about 34°C. Repeated scans over larger areas exceeding 40,000 μm^2 revealed similar structures and confirmed the above conclusion. The small 'islands' in the interfacial region indicate

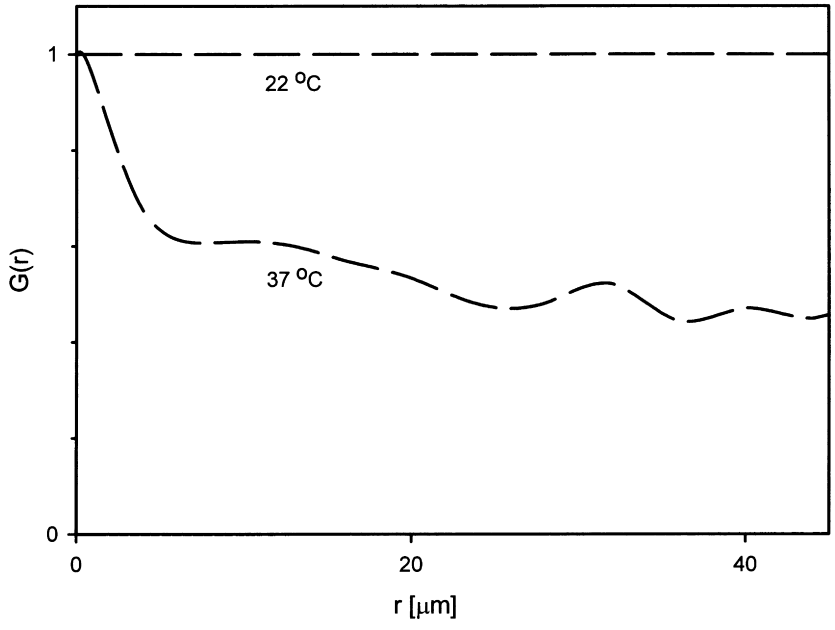

Fig. 4. Density correlation functions for the bulk NIPA gel at 22 and 37°C.

formation of microdomains at the phase separation region. Those 'islands' are probably responsible for the increase of gel turbidity [12], as well as increase of ultrasonic attenuation [13] as temperature increases above T_c. It is also seen that the density of the gel increases near the surface.

The density of NIPA versus distance across the interface at $T = 37°C$ is shown in Fig. 2(b). It is seen that at $T > T_c$ the interfacial profile exhibits a peak, indicating the formation of a dense skin. The change of the interfacial polymer concentration from the maximum to zero can be well described by the Gaussian distribution function, Eq. (1). A similar decay was observed at room temperature. However, average interface thickness for the high-temperature phase is increased to 65 ± 13 μm.

In Fig. 3 we compare the distribution of the interface thickness along the interface at 22 and 37°C. For the relatively small section of the surface, at low temperature the correlation depth varies widely from 18 to 60 μm, but at high temperature that range is much smaller, from 55 to 78 μm.

We also mapped the polymer distribution within the bulk gel. Images similar to those depicted in Figs. 1 and 2 were obtained, this time, however, not in the direction perpendicular to the interface but in the plane parallel to the surface. From Figs. 1 and 2 one observes that the water–gel interface is rough and it is difficult to define the surface. In a series of experiments we deliberately focused the laser about 25 μm below the level corresponding to the fully dense gel, i.e. below the contours labeled in Figs. 1 and 2 as 100. During the mapping of an area of 400×400 μm^2 the Raman signal was collected from a small section of the volume illuminated by the laser approximated by a cylinder 0.5 μm in diameter and 4 μm tall. These experiments reveal the advantage of the Raman technique over the atomic force microscopy (AFM). AFM cannot characterize the density distribution along the direction perpendicular to the interface and within the bulk of the gel. The images yielded sufficient amount of data to calculate the density correlation functions defined as

$$G(r) = \langle I(r_0)I(r + r_0)\rangle / \langle I(r_0)^2\rangle \quad (2)$$

where $I(r)$ is the intensity of the Raman band at 1445 cm^{-1}. In Fig. 4 we compare correlation functions $G(r)$ obtained at room temperature and at 37°C by mapping the interior of the gel when the laser was focused some 25 μm below the top surface of the gel. The density correlation function is equal to one and this value is constant, indicating the bulk gel has a homogeneous structure at room temperature. The gel becomes inhomogeneous at 37°C as indicated by the decrease of the correlation function.

Above observations clearly show that both the interface and bulk properties of the NIPA gel drastically change when the temperature is increased from room temperature (below T_c) to 37°C (above T_c). They may be summarized as follows: (1) the NIPA gel has a rougher interface at room temperature than at 37°C; (2) the interface thickness at room temperature is smaller compared to that measured at 37°C; and (3) the interior structure of the NIPA gel is homogeneous at room temperature, but becomes heterogeneous at 37°C. These observations may be understood by considering nature of the molecular structure of the NIPA gel.

It is well known that at room temperature the NIPA gel is hydrophilic, and water molecules surround and hydrate the NIPA polymer network [5]. The gel therefore swells in the surrounding water and becomes homogeneous and transparent. It is the hydrophilic property of the NIPA gel that leads to an increase of the gel surface, i.e. rougher surface. At 37°C, on the other hand, the intrinsic affinity of NIPA polymer chains for themselves is enhanced due to thermal dissociation of hydrating water molecules from the polymer network [8]. Due to hydrophobic interaction, the gel tends to repel excess water out of its network. Since the water in the surface area can easily diffuse out to the external water reservoir, the interface of the gel becomes dense. The interior of the sample is under constant volume condition, i.e. the thermodynamic path is an isochore (constant volume). As a result, the system stays inside the unstable zone and starts to decompose into dense and dilute domains with different network concentrations [6,12]. As directly seen in Fig. 2(a), the small islands in the contour plot of the NIPA gel at 37°C represent such microdomains that cause the heterogeneous structure, resulting in the decrease of the correlation function as shown in Fig. 4. At 37°C the interface is smoother relative to what we observed at room temperature. This is the direct result of the tendency of the system to minimize its hydrophobic interaction energy by reducing the size of the gel–water interface.

The increase of the interfacial thickness may be due to the formation of a dense surface shell during the shrinking process [6]. In our measurement, the gel was quickly heated to above T_c and measured within about 30 min. Under this condition, the excess of water inside the gel cannot be expelled quickly. On the other hand, the polymer network at the gel surface can respond to the temperature rise quickly and forms a dense layer impermeable to the inner water. It is noted that the interfacial profiles observed in this study are in the range from 10 to 100 μm. The interface profile may be viewed over a much shorter length scale by X-ray and neutron reflectivity measurements which have been used for study of adsorption at the solid–liquid interface [14–17]. For example, Lee et al. [16] observed that up to the distance of about 10 nm, polymer density varies near the interface as $z^{-4/3}$. They attributed this effect to surface tension and postulated strong adsorption and weak coupling. Schlossman and coworkers [17] used X-ray reflectivity and observed similar density profiles as that depicted in Fig. 2(b). However, they were able to determine the density profile on a very short range of a couple of tens of nanometers.

4. Conclusions

The interfacial thickening and smoothing of the NIPA hydrogel that undergoes the volume phase transition has been directly observed by Raman microimaging technique. The thickening effect may be due to the formation of the dense shell during the shrinking process, while the smoothing is due to hydrophobic interaction between isopropyl groups in the NIPA gel as the sample undergoes the volume phase transition. Measuring the interface profile as a function of crosslinker concentration and gel thickness will be an important topic of further studies. Furthermore, it is demonstrated that this nondestructive method is uniquely suited to characterizing the interfacial profiles of hydrogels and could open new avenues for better understanding this unique class of macromolecular materials.

Acknowledgements

Acknowledgement is made to the Donors of the Petroleum Research Fund, administered by the American Chemical Society, and to the US Army Research Office under Grant No. DAAG55-98-1-0175, for partial support of this research.

References

[1] Ratner BD. In: Ratner BD, Hoffman AS, Schoen FJ, Lemons JE, editors. Biomaterials science. San Diego, CA: Academic Press, 1996. p. 21.
[2] Peppas NA. Hydrogel in medicine and pharmacy. Boca Raton, FL: CRC Press, 1987.
[3] Tanaka T. Phys Rev Lett 1978;40:820.
[4] Tanaka T. Sci Am 1981;244:124.
[5] Hirotsu S, Hirokawa Y, Tanaka T. J Chem Phys 1987;87:1392.
[6] Matsuo ES, Tanaka T. J Phys Chem 1988;89:1695.
[7] Matsuo ES, Tanaka T. Nature 1992;358:482.
[8] Li C, Hu Z, Li Y. J Chem Phys 1994;100:4645.
[9] Park TG, Hoffman AS. Biotechnol Prog 1994;10:32.
[10] Suzuki A, Yamazaki M, Kobiki Y. J Chem Phys 1996;104: 1751.
[11] Appel R, Xu W, Zerda TW, Hu Z. Macromolecules 1998;31: 5071.
[12] Li Y, Wang G, Hu Z. Macromolecules 1995;28:4194.
[13] Yuan K, Hu Z, Li Y. Appl Phys Lett 1999;74:2233.
[14] Rennie AR, Lee EM, Simister EA, Thomas RK. Langmuir 1990;6:1031.
[15] Cosgrove T, Heath TG, Phipps JS, Richardson RM. Macromolecules 1991;24:94.
[16] Lee TE, Guiselin O, Farnoux B, Lapp A. Macromolecules 1991;24:2518.
[17] Schlossman ML, Schwartz DK, Kawamato EH, Kellogg GJ, Pershan PS, Kim MW, Chung TC. J Phys Chem 1991;95:6628.